

## Effect of Y on Formation of Hard Magnetic Phases in Fe-Matrix Alloys

B. JEŹ<sup>a,\*</sup>, K. BŁOCH<sup>a</sup>, J. GONDRO<sup>a</sup>, K. JEŹ<sup>a</sup>,  
M. TALAR<sup>a</sup>, B. PŁOSZAJ<sup>a</sup>, P. PIETRUSIEWICZ<sup>a</sup>,  
S. WALTERS<sup>b</sup>, A. KALWIK<sup>c</sup>, D.S. CHE HALIN<sup>d</sup>,  
P. SIKORA<sup>c</sup> AND M. NABIAŁEK<sup>a</sup>

<sup>a</sup>*Department of Physics, Częstochowa University of Technology,  
al. Armii Krajowej 19, 42-200 Częstochowa, Poland*

<sup>b</sup>*Advanced Engineering Centre, University of Brighton, BN2 4GJ, Brighton, United Kingdom*

<sup>c</sup>*Department of Technology and Automation, Faculty of Mechanical Engineering and Computer Science, Częstochowa University of Technology,  
al. Armii Krajowej 19, 42-200 Częstochowa, Poland*

<sup>d</sup>*Centre of Excellence Geopolymer and Green Technology (CEGeoGTech),  
Universiti Malaysia Perlis (UniMAP), 01000 Kangar, Perlis, Malaysia*

Doi: [10.12693/APhysPolA.139.495](https://doi.org/10.12693/APhysPolA.139.495)

\*e-mail: [bartek199.91@o2.pl](mailto:bartek199.91@o2.pl)

In this work, the structural and magnetic properties of rapidly-cooled alloys  $\text{Fe}_{60}\text{Co}_{10}\text{Y}_{5+x}\text{Zr}_{5-x}\text{B}_{20}$  were investigated. The chemical composition of the alloy and manufacturing parameters were selected to obtain a partially-crystallised structure. The tested nanocrystalline alloys were produced by injection of each liquid alloy into a copper mould. The structure of each alloy was investigated using X-ray diffraction. The diffractogram analysis was performed using the specialist Match! software. The magnetic properties of the alloys were determined on the basis of measurements that were carried out using a vibrating sample magnetometer. The study showed that it is possible, using a single-stage process, to produce an alloy with a nanocrystalline structure containing a significant proportion of an amorphous matrix. It was found that varying the proportions of Y and Zr promoted the creation of different crystalline phases. This fact was related to the physical properties of the elements: the higher value of the negative heat of mixing for Zr with the other alloying components, compared with Y. In the case of the alloy with the higher content of Y, a phase was identified which exhibited so-called “hard-magnetic” properties. The formation of this phase results in a different distribution of Fe atoms, as indicated by a higher value of saturation magnetisation and lower value of the spin-wave stiffness parameter.

topics: rapidly-quenched alloys, X-ray diffractometry, hard magnetic phases, injection-casting method

### 1. Introduction

Rapidly-cooled partially-crystallised alloys, that are based on an Fe matrix, exhibit good magnetic properties. Depending on the composition and type of structure, these alloys may have semi-hard or hard magnetic properties. Crystalline phases are responsible for such properties, for example,  $\text{Co}_5\text{Y}$ ,  $\text{Fe}_5\text{Y}$ ,  $\text{YFe}_{14}\text{B}_2$  [1]. The atomic radii and values of the mutual heat of mixing of the individual alloy components are two of several important parameters which determine the chemical composition of the alloy. According to the criteria of A. Inoue [2], an alloy has a promising glass transition ability if the differences in the atomic radii lengths are sufficiently large, and if there is a negative heat of mixing between the components.

One of the most promising groups of amorphous and nanocrystalline alloys are alloys based on Fe–B. The glass transition ability of these alloys can be modified by the use of alloying additives, usually involving transition metals: Mo, Zr, Hf, Cr, Y, Nb, and non-metals: such as P or C [3–8]. The appropriate selection of the chemical composition enables the production of samples with thicknesses that can exceed 10 mm [9, 10]. The deliberate reduction of an alloy’s glass transition ability, through changes in the chemical composition and careful selection of the cooling rate, enables the production of an alloy with a partially-crystalline structure in a one-stage production process.

The aim of this work was to investigate the effect of the addition of Y, at the expense of Zr, on the formation of semi-hard and hard magnetic phases in

rapidly-cooled alloys based on Fe matrix, and which are produced in a single-stage production process.

## 2. Materials and methods

The investigated polycrystalline alloys,  $\text{Fe}_{60}\text{Co}_{10}\text{Y}_{5+x}\text{Zr}_{5-x}\text{B}_{20}$ , were produced in an electric arc furnace; component elements of the following purities were used: Fe — 99.98%, Co — 99.99%, Zr — 99.9%, Y — 99.95%, B — 99.9%. The melting process was carried out under a protective argon atmosphere. The smelting process was repeated five times for enhanced mixing of the component elements. Ingots were cleaned mechanically, divided into smaller pieces, and then subjected to further cleaning in an ultrasonic cleaner. Rapidly-cooled alloys were then made by injection casting. The charge was placed in a quartz crucible and melted using induction heating. The liquid melt was forced, under argon pressure, into the copper mould. Rod-shaped samples were produced, each with a length of 20 mm and diameter of 1 mm. The production process was carried out under a protective argon atmosphere.

The structure of the produced alloys was examined using a Bruker D8 Advance diffractometer. The measurements were performed on powdered samples (the alloys were pulverised inside an agate mortar). The tests were conducted over the range of  $30\text{--}100^\circ$  of the  $2\theta$  angle.

The magnetic properties were studied using a LakeShore vibration magnetometer. Measurements were carried out in the range of external magnetic field up to 2 T. Primary magnetisation curves and static magnetic hysteresis loops were recorded.

## 3. Results

Figure 1 shows the X-ray diffraction images measured for the tested alloys. The diffractograms show wide maxima in the range of  $40\text{--}50^\circ$  of  $2\theta$  angle. In each case, this maximum indicates the presence of a disordered phase within the volume of the alloy. The X-ray diffraction images also show narrow peaks of significant intensity. Their presence proves the existence of ordered phases within the volumes of the produced materials. By using specialist software (i.e., Match!), analysis was performed on the diffractograms and crystal phases were identified. In the case of the  $\text{Fe}_{60}\text{Co}_{10}\text{Y}_5\text{Zr}_5\text{B}_{20}$  alloy:  $\text{CoZr}$  and  $\text{Fe}_2\text{B}$  were detected; and for the  $\text{Fe}_{60}\text{Co}_{10}\text{Y}_6\text{Zr}_4\text{B}_{20}$  alloy:  $\text{Co}_5\text{Y}$ ,  $\text{BCo}_2$  and  $\text{Fe}_2\text{B}$  were identified. The effect of the Zr and Y content on the formation of crystalline phases can be seen. Zirconium is characterised by significantly higher values of negative heat of mixing with alloying components as compared to yttrium: (Zr–Co — 41, Y–Co — 22; Zr–B — 71, Y–B — 50; Zr–Fe — 25, Y–Fe — 1) [2]. The addition of Y (the element with less influence on the glass transition ability) results in the formation of more crystalline phases, including the hard-magnetic  $\text{Co}_5\text{Y}$  phase.

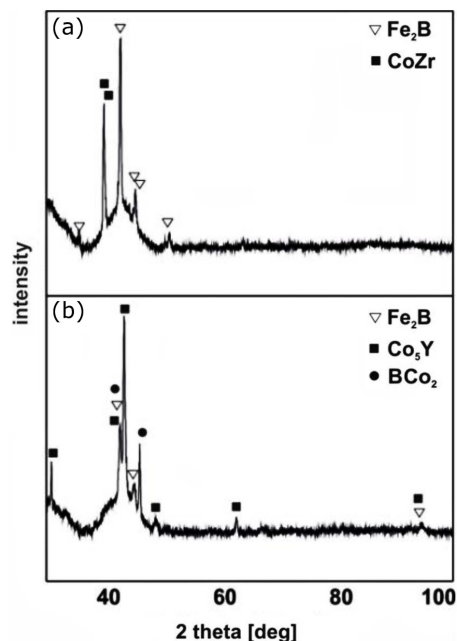


Fig. 1. X-ray diffraction patterns for the alloy samples: (a)  $\text{Fe}_{60}\text{Co}_{10}\text{Y}_5\text{Zr}_5\text{B}_{20}$ , (b)  $\text{Fe}_{60}\text{Co}_{10}\text{Y}_6\text{Zr}_4\text{B}_{20}$ .

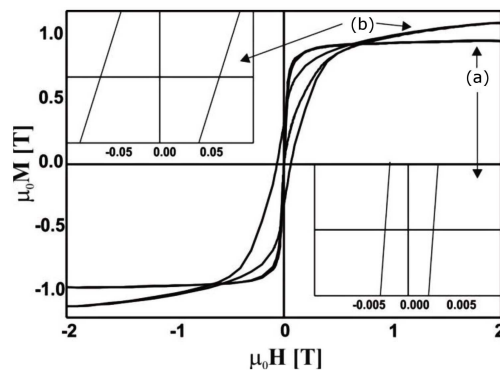


Fig. 2. Static magnetic hysteresis loops for the alloys: (a)  $\text{Fe}_{60}\text{Co}_{10}\text{Y}_5\text{Zr}_5\text{B}_{20}$ , (b)  $\text{Fe}_{60}\text{Co}_{10}\text{Y}_6\text{Zr}_4\text{B}_{20}$ .

Figure 2 shows static magnetic hysteresis loops for the tested alloys. The recorded hysteresis loops have different characteristic shapes. The loop for the  $\text{Fe}_{60}\text{Co}_{10}\text{Y}_5\text{Zr}_5\text{B}_{20}$  alloy features a shape that is typical for a soft ferromagnetic material. This alloy undergoes the process of magnetisation much more easily than in the case of the  $\text{Fe}_{60}\text{Co}_{10}\text{Y}_6\text{Zr}_4\text{B}_{20}$  alloy. In the case of the latter  $\text{Fe}_{60}\text{Co}_{10}\text{Y}_6\text{Zr}_4\text{B}_{20}$  alloy, the primary magnetisation curve is much more inclined towards the axis  $\mu_0 H$  and the magnetisation reaches its saturation value in a magnetic field with a much higher value. The loop recorded for the  $\text{Fe}_{60}\text{Co}_{10}\text{Y}_6\text{Zr}_4\text{B}_{20}$  alloy is clearly wider, and this is related to the presence of the crystalline  $\text{Co}_5\text{Y}$  phase grains exhibiting hard-magnetic properties. Based on the paths traced by the static magnetic hysteresis loops, values were determined for the  $H_C$  coercive field and the  $M_S$  saturation magnetisation.

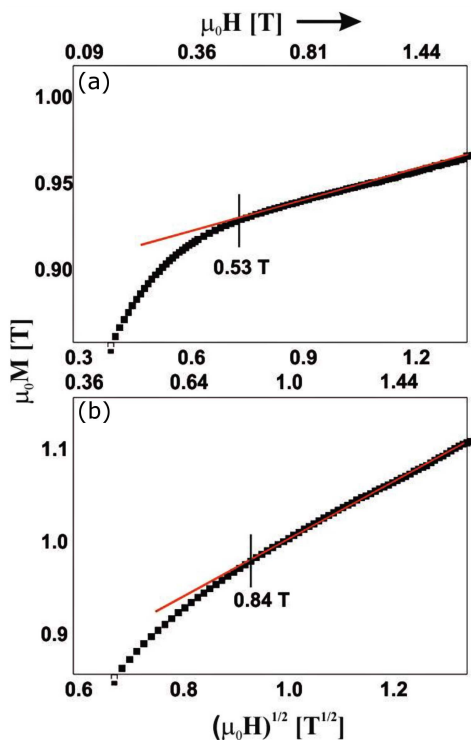


Fig. 3. Magnetisation curves as a function of  $(\mu_0 H)^{1/2}$  for the alloy samples: (a)  $\text{Fe}_{60}\text{Co}_{10}\text{Y}_5\text{Zr}_5\text{B}_{20}$ , (b)  $\text{Fe}_{60}\text{Co}_{10}\text{Y}_6\text{Zr}_4\text{B}_{20}$ .

In the case of the  $\text{Fe}_{60}\text{Co}_{10}\text{Y}_5\text{Zr}_5\text{B}_{20}$  alloy:  $H_C = 2050$  A/m,  $M_S = 0.97$  T; for the  $\text{Fe}_{60}\text{Co}_{10}\text{Y}_6\text{Zr}_4\text{B}_{20}$  alloy one has  $H_C = 50000$  A/m,  $M_S = 1.11$  T. The magnetisation process in high magnetic fields was analysed for the tested alloys. Figure 3 presents the magnetisation curves as a function of  $(\mu_0 H)^{1/2}$ .

Analysis of the initial magnetisation curve, in the Holstein–Primakoff paraprocess region, allows the determination of a parameter describing the stiffness of the spin-wave ( $D_{\text{spf}}$ ) [11–13]. The parameter  $D_{\text{spf}}$  is related with coefficient  $b$  by the relation

$$b = 3.54\mu_0 \left( \frac{g\mu_B}{4\pi D_{\text{spf}}} \right)^{\frac{3}{2}} k_B T, \quad (1)$$

where  $b$  — the slope of the linear fit corresponding to the thermally-induced suppression of spin-waves by a magnetic field of high intensity,  $\mu_0$  — the magnetic permeability of a vacuum,  $k_B$  — the Boltzmann’s constant,  $\mu_B$  — the Bohr magneton,  $g$  — the gyromagnetic factor,  $T$  — the temperature.

TABLE I

Magnetic properties of the  $\text{Fe}_{60}\text{Co}_{10}\text{Y}_{5+x}\text{Zr}_{5-x}\text{B}_{20}$  alloys and the identified crystalline phases.

	$M_S$ [T]	$H_C$ [A/m]	$D_{\text{spf}}$ [meV nm <sup>2</sup> ]	phases
$\text{Fe}_{60}\text{Co}_{10}\text{Y}_5\text{Zr}_5\text{B}_{20}$	0.97	2050	43	CoZr, Fe <sub>2</sub> B
$\text{Fe}_{60}\text{Co}_{10}\text{Y}_6\text{Zr}_4\text{B}_{20}$	1.11	50000	15	Co <sub>5</sub> Y, BCo <sub>2</sub> , Fe <sub>2</sub> B

Table I contains the determined magnetic properties and the identified crystal phases for the tested alloys. A significant decrease in the  $D_{\text{spf}}$  parameter was noted in the case of the alloy with the higher Y content. This can be related to the change in the distance between the pairs of magnetic atoms: Fe–Fe, Fe–Co, and Co–Co. This, in turn, is caused by the presence of the Co<sub>5</sub>Y crystalline phase in the tested alloy.

#### 4. Conclusions

The aim of this study was to determine the effect of the addition of Y, at the expense of Zr, on the formation of phases with hard-magnetic properties. It was found that a slight change in the chemical composition of the alloy influenced the course of the crystallisation process. An addition of just 1% of Y, at the expense of Zr, contributed to the formation of the hard-magnetic Co<sub>5</sub>Y phase. Interestingly, different phases were identified for the alloy with the higher Y content as compared with the alloy with the equilibrium content of Y and Zr. The differing processes of atomic diffusion, during the solidification of the alloys, could be associated with the value of the mixing heat of the alloying elements. In comparison with Y, Zr is characterised by a higher value of negative heat of mixing with other alloying elements. The addition of Y, at the expense of Zr, reduces the glass transition ability of the alloy and changes the distribution of Fe and Co atoms, thereby changing the distance between them. This is indicated by a significant reduction in the value of the  $D_{\text{spf}}$  parameter. The properties of the examined alloys are related closely to their structure. The appearance of a phase with hard-magnetic properties significantly increased the value of the coercive field and altered the course of the magnetisation process.

The results of this research indicate that the appropriate design of the manufacturing process, and careful selection of the chemical composition, can lead to the production of nanocrystalline alloys with hard-magnetic properties, using a single-stage production process.

#### References

- [1] P. Vizureanu, M. Nabiałek, A.V. Sandu, B. Jeż, *Materials* **13**, 835 (2020).
- [2] A. Takeuchi, A. Inoue, *Mater. Trans.* **46(12)**, 2817 (2005).
- [3] M.E. Mchenry, M.A. Willard, D.E. Laughlin, *Prog. Mater. Sci.* **44**, 291 (1999).
- [4] Z. Jaafari, A. Seifoddini, S. Hasani, *Metall. Mater. Trans. A* **50A**, 2875 (2019).
- [5] P. Pietrusiewicz, M. Nabiałek, B. Jeż, *Rev. de Chim.* **69(8)**, 2097 (2018).
- [6] M.S. Baltatu, C.A. Tugui, M.C. Perju, M. Benchea, M.C. Spataru, A.V. Sandu, P. Vizureanu, *Rev. de Chim.* **70**, 1302 (2019).

- [7] M.G. Minciuna, P. Vizureanu, V. Geanta, I. Voiculescu, A.V. Sandu, D.C. Achitei, A.M. Vitalariu, *Rev. de Chim.* **66**, 891 (2015).
- [8] A.V. Sandu, A. Ciomaga, G. Nemtoi, C. Bejinariu, I. Sandu, *J. Optoelectron. Adv. Mater.* **14**, 704 (2012).
- [9] P. Rezaei-Shahreza, A. Seifoddini, S. Hasani, *J. Alloys Compd.* **738**, 197 (2018).
- [10] S. Hasani, P. Rezaei-Shahreza, A. Seifoddini, *Metall. Mater. Trans. A* **50**, 63 (2019).
- [11] T. Holstein, H. Primakoff, *Phys. Rev.* **58**, 1098 (1940).
- [12] J. Gondro, K. Błoch, M. Nabiałek, S. Garus, *Mater. Tehnol.* **50**, 559 (2016).
- [13] K. Błoch, *Rev. de Chim.* **69**, 982 (2018).